APPLIED GEOPHYSICS, Vol.15, No.1 (March 2018), P.57-68, 9 Figures.
DOI:10.1007/s11770-018-0660-2

Study and application of PS-wave pre-stack migration in HTI media and an anisotropic correction method*

YanLi-Li[1,2], Cheng Bing-Jie♦[1,3], Xu Tian-Ji[4,5], Jiang Ying-Ying[4,5], Ma Zhao-Jun[4,5], and Tang Jian-Ming[5,6]

Abstract: Anisotropy correction is necessary during the processing of converted PS-wave seismic data to achieve accurate structural imaging, reservoir prediction, and fracture detection. To effectively eliminate the adverse effects of S-wave splitting and to improve PS-wave imaging quality, we tested methods for pre-stack migration imaging and anisotropic correction of PS-wave data. We based this on the propagation rules of seismic waves in a horizontal transverse isotropy medium, which is a fractured medium model that reflects likely subsurface conditions in the field. We used the radial (R) and transverse (T) components of PS-wave data to separate the fast and slow S-wave components, after which their propagation moveout was effectively extracted. Meanwhile, corrections for the energies and propagation moveouts of the R and T components were implemented using mathematical rotation. The PS-wave imaging quality was distinctly improved, and we demonstrated the reliability of our methods through numerical simulations. Applying our methods to three-dimensional and three-component seismic field data from the Xinchang-Hexingchang region of the Western Sichuan Depression in China, we obtained high-quality seismic imaging with continuous reflection wave groups, distinct structural features, and specific stratigraphic contact relationships. This study provides an effective and reliable approach for data processing that will improve the exploration of complex, hidden lithologic gas reservoirs.
Keywords: HTI media, PS-wave, pre-stack time migration, anisotropic correction, Xinchang-Hexingchang region, the Western Sichuan Depression

Introduction

Anisotropy may form within subsurface media as a result of matrix arrangement, fluid permeation, and the characteristics of pores, cracks, or fractures therein. Thus, the numerous dynamic, kinematic, and geometrical attributes, such as amplitude, frequency, propagation velocity, dispersion, and attenuation, of seismic waves may azimuthally vary while propagating

Manuscript received by the Editor May 28, 2017; revised manuscript received February 7, 2018.
*This work was supported by the National Natural Science Foundation of China (Grant No. 41574099) and the National Key Science and Technology Special Projects (grant No. 2016ZX05002004-005).
1. State Key Laboratory of Oil and Gas Reservoir Geology and Exploitation, Chengdu University of Technology, Chengdu 610059, China.
2. College of Earth Science, Chengdu University of Technology, Chengdu 610059, China.
3. College of Geophysics, Chengdu University of Technology, Chengdu 610059, China.
4. Exploration& Production Institute, Southwest Oil & Gas Company, SINOPEC, Chengdu 610041, China.
5. Key Lab of Multiple Wave Seismic Technology, SINOPEC, Chengdu 610041, China.
6. Southwest oil and gas Branch Company. SINOPEC, Chengdu 610041, China.
♦Corresponding author: Cheng Bing-Jie (Email: chengbingjie09@cdut.cn)

through anisotropic media, so multiple methods have been developed to analyze seismic anisotropy. Multi-wave amplitude variation with azimuths and velocity variation with azimuths, as well as shear wave splitting, have shown promising results (Cheng and Xu, 2009; Akalin et al., 2014; Zhang et al., 2015).

Research on migration imaging of PS-waves has gained increasing attention in recent years. Sun and Martinez (2003) investigated a PS-wave migration processing method with a 3D, true-amplitude weighting function based on Schleicher's theory. Li et al. (2005) and Dai et al. (2005, 2006, 2007a, 2007b, 2008b) applied a 4-parameter PS-wave Kirchhoff migration processing technique to several types of strata, including homogeneous and multi-layered media, based on a precise velocity analysis. In addition, Zhang et al. (2009) researched the true-amplitude, pre-stack migration of PS-waves, based on a virtual offset. Huang et al. (2009, 2014) achieved the 3D true-amplitude anisotropy Kirchhoff migration of PS-waves based on layered media and Bleistein's theory. Based on the 4-parameter migration method described by Dai and Li (2005, 2008b), Li et al. (2013) and Chen et al. (2016) each developed a pre-stack migration method for the 2-parameter simplified equation for vertical transverse isotropy (VTI) media.

Despite this extensive effort, PS-wave imaging research has remained focused on the propagation of PS-waves through isotropic, homogeneously layered, or VTI media, and the field has largely neglected the fact that PS-waves are even more sensitive to anisotropy than simple P-waves (Qian et al., 2012). Anisotropy can directly lead to the PS-wave propagation moveout, which causes adverse effects during the processing of wide-azimuth PS-wave data (e.g., velocity analysis, normal moveout correction, and dip moveout correction), giving rise to false structural artifacts that are particularly detrimental to the identification and analysis of fine structures (Li et al., 2015). For example, the propagation time and amplitude of the radial (R) component of a PS-wave changes notably with the azimuth, whereas the transverse (T) component exhibits an obvious polarity reversal at every azimuth multiple of 90°. It is therefore necessary to apply effective corrections to eliminate the influences of imaging effects.

Anisotropy also provides direct evidence for the existence of cracks with the target media. Removing it is somewhat controversial because its retention during the processing of converted-wave data can enable useful insights. Recent studies on PS-wave seismic data have suggested that the decision to retain or eliminate anisotropy should depend on the specific geological target. Jenner (2011) presented a pre-stack time migration method for P-wave data that combined VTI and horizontal transverse isotropy (HTI) media; he then discussed an effective workflow and demonstrated it with examples. Cheng et al. (2012) achieved pre-stack migration imaging while preserving anisotropic features within VTI media in the angle domain. Koren and Ravve (2014) also proposed a velocity updating method for anisotropic processing. The general consensus is that to obtain the high-quality, converted-wave, fast S-wave and slow S-wave seismic data that are necessary for effective multi-wave and multi-component seismic exploration (Dai and Li, 2011), anisotropy effects on energy, moveout, and frequency of PS-wave data must be eliminated (Cheng et al., 2012; Simmons, 2009).

Currently, few cases have successfully solved the PS-wave imaging problem in fractured media under actual, complex geological conditions. Instead, most studies have been based on forward modeling with theoretical or synthetic data. To conduct a structural and stratigraphic interpretation and to extract amplitude versus offset (AVO) response characteristics, the anisotropy and S-wave splitting phenomena within the fractured media must be treated for PS-wave pre-stack trace gathers and post-stack imaging. The effects of anisotropy must be eliminated before the analysis can accurately identify lithological or oil-gas anomalies when using PS-wave data for AVO inversion or AVO analysis (Skopintseva and Alkhalifah, 2013). This is because the reflection amplitude of a PS-wave that is propagating through a fractured medium simultaneously changes with the azimuth and offset (Mahmoudian et al., 2015; Chang et al, 2017). However, the anisotropic features in seismic data should be retained when S-wave splitting phenomena are being employed to detect fractures.

In this study, we analyzed PS-wave propagation characteristics in HTI media and investigated a pre-stack time migration and anisotropic correction method based on HTI media and S-wave splitting. The reliability of the proposed method was verified through HTI-media forward modeling, after which the method was applied to a real-world, ultra-deep (more than 5000 m), ultra-tight, low-porosity, and low-permeability gas reservoir with strong heterogeneity and anisotropic features in the Xinchang-Hexingchang region of the Western Sichuan Depression. The results included high-quality PS-wave R and T component data, as well as fast and slow S-wave seismic data, which could prove highly useful for improving future structural interpretations, strata tracking precision, and fracture detection.

Methodology and technological realization

Seismic numerical simulation of HTI media and wave field features

Real subsurface media are commonly characterized by multi-phase heterogeneities, partial elasticity, and anisotropy. Hexagonally symmetrical anisotropic media have been studied more than other types. They primarily include transversely isotropic media that are characterized by vertical transverse isotropy with a vertical axis of symmetry (i.e., VTI), horizontal transverse isotropy with a horizontal axis of symmetry (i.e., HTI), or transverse isotropy with a tilted axis of symmetry (TTI; Thomsen, 1986; Thomsen 1999; Berryman, 2009). An HTI medium (which is azimuthally anisotropic) is considered to be a good representation of subsurface vertically fractured media (Thomsen, 1986). Vertical fractures serve as both favorable storage elements and important migration channels for oil and gas (Mahmoudian et al, 2015; Chang et al, 2017). Therefore, it is vitally important to identify the development areas, principle directions, and densities of such fractures during seismic exploration, especially when planning well deployment and well trajectory.

When a seismic wave propagates through HTI media, the directional distributions of fractures or joints, the depositional patterns of rock strata, and the directional alignments of stress fields can all lead to anisotropy within the velocity, time, amplitude, energy, and frequency of the seismic wave. S-waves are particularly sensitive to such anisotropy, and S-wave splitting can add even more complexity (Skopintseva and Alkhalifah, 2013). When propagating through an anisotropic medium (e.g., a fractured medium), an S-wave will split into fast and slow S-waves with orthogonal polarizations parallel and perpendicular to the fracture strike, respectively. The former will propagate faster than the latter. Since such splitting only occurs when an S-wave propagates at a certain angle relative to a fracture, the intensities of the split fast and slow S-waves are closely related to the fracture dimensions (Crampin and Peacock, 2005; Koren and Ravve, 2014). These characteristics can be observed and analyzed through numerical simulations.

Table 1 lists the parameters of the simulated multi-layer HTI fractured medium that we used in our model. There were seven layers in total and the second, fourth, and sixth layers were set as fractured, anisotropic layers (Table 2). In the numerical simulation, the detection points were set at 36 azimuths, at a step of 10°, and with a geophone interval of 1000 m. The changing features of the P-wave (vertical or Z-component) and the PS-waves (horizontal or X- and Y-components) at each azimuth were obtained (Figure 2).

Table 1 Parameters of forward modeling numerical simulation

Formation No.	Formation	Density (g/cm3)	P-wave velocity (km/s)	S-wave velocity (km/s)	Depth (m)
1	Isotropic layer/mudstone	2.46	3.708	1.942	0–1000
2	HTI medium layer/sandstone	2.54	4.433	3.047	1000–1150
3	Isotropic layer/mudstone	2.57	4.719	2.176	1150–1650
4	HTI medium layer/sandstone	2.61	5.046	3.310	1650–1850
5	Isotropic layer/mudstone	2.6	5.193	2.385	1850–2350
6	HTI medium layer/sandstone	2.6	5.35	3.667	2350–2650
7	Isotropic half-space/sandstone	2.67	5.55	2.542	2650–…

Table 2 Model parameters of the HTI media

HTI-media layer	Fracture strike (°)	Radius (m)	Aspect ratio	Density of filling gas (g/cm^3)
2	60	0.001	0.01	0.05
4	45	0.001	0.01	0.08
6	20	0.001	0.01	0.15

PS-wave pre-stack migration

Figure 1 displays the changes of the seismic amplitudes for the X, Y, and Z components at each azimuth. It clearly shows the waves reflected from each of the six interfaces. The reflection wave events for the Z- and X-components along the first isotropic interface exhibit no azimuthal anisotropy. Meanwhile, the Y-component shows no energy at the first isotropic interface, but it exhibits a strong response along the anisotropic interfaces. In addition, a polarity reversal can be observed in the Y-component response. These features confirm that converted waves in HTI media are characterized by azimuthal anisotropy and that PS-waves will split into fast and slow S-wave components.

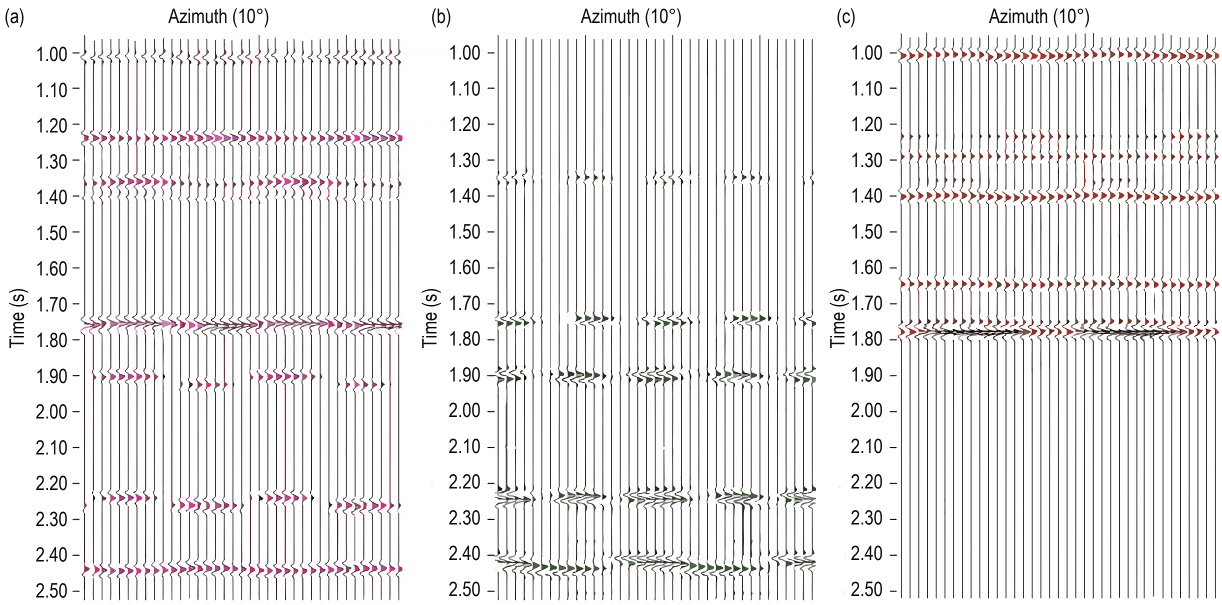

Fig. 1 Three component simulated records of HTI medium. X-component (a), Y-component (b), Z-component (c).

Converted-wave pre-stack time migration method based on HTI media

The estimated velocity changes in the subsurface were fitted by compensating for azimuthal anisotropy during the pre-stack migration processing of PS-wave seismic data (Dai and Li, 2008a). These fitted velocity-variation estimates were then synthesized into a velocity ellipse, the orientations of which were employed to conduct dynamic correction stacking. For pre-stack time migration, the travel time of a converted wave, t_{ps}, can be expressed in terms of the P-wave travel time, t_p, and the S-wave travel time, t_s, as $t_{ps} = t_p + t_s$, where t_p and t_s is approximately expressed as

$$t_p = \frac{1}{1+\gamma_0}\sqrt{t_{ps0}^2 + \frac{\chi_p^2(1+\gamma_0)(1+\gamma_{eff})}{v_{ps}^2\gamma_{eff}} - \frac{2\eta_{eff}\left[\chi_p^2\left(1+\gamma_0\right)\left(1+\gamma_{eff}\right)\right]^2}{v_{ps}^2\gamma_{eff}\left[t_{ps0}^2 v_{ps}^2\gamma_{eff} + \left(1+2\eta_{eff}\right)\chi_p^2\left(1+\gamma_0\right)\left(1+\gamma_{eff}\right)\right]}} \quad (1)$$

$$t_s = \frac{\gamma_0}{1+\gamma_0}\sqrt{t_{ps0}^2 + \frac{\chi_s^2\left(1+\gamma_0\right)\left(1+\gamma_{eff}\right)}{v_{ps}^2\gamma_0} - \frac{2\xi_{eff}\left[\chi_s^2\left(1+\gamma_0\right)\left(1+\gamma_{eff}\right)\right]^2}{v_{ps}^2\gamma_0\left[t_{ps0}^2 v_{ps}^2\gamma_0 + \chi_s^2\left(1+\gamma_0\right)\left(1+\gamma_{eff}\right)\right]}}\,. \quad (2)$$

Suppose that the PS-wave velocity is the most sensitive parameter in equations (1) and (2), where t_{ps} is the travel time of the converted wave, t_p is the P-wave travel time, t_p is the S-wave travel time, γ_0 is the ratio of the vertical P-wave velocity to that of the S-wave, t_{ps0} is the zero-offset converted-wave travel time, χ_p is the distance from the shot to the image point, χ_s is the distance from the image point to the receiver, γ_{eff} is the effective velocity ratio, v_{ps} is the PS-wave velocity (a combination of the P- and S-wave velocities), η_{eff} is the effective P-wave anisotropy parameter, and ξ_{eff} is the S-wave anisotropy parameter. For a weakly anisotropic medium, the anisotropic variations in γ_{eff} and χ_{eff} can safely be ignored, so that only the anisotropic change in velocity is considered (Li and Yuan, 2003). The anisotropic velocity variation is equivalent to the anisotropic variation in the stacked velocity.

Our pre-stack time migration processing of PS-waves that were propagating through HTI media comprised six steps (Dai et al., 2004; Jenner, 2011).

(1) Offset setup: generally, the maximum vertical offset was taken as the limit so that each azimuth had the same maximum offset, which prevented azimuthal velocity variations due to differences in the data.

(2) Full-azimuth migration velocity analysis: the migration velocities and azimuthal parameters were obtained through full azimuthal seismic data migration velocity analysis.

(3) Azimuth selection: using due north as the starting azimuth, an azimuthal selection process was conducted for super-gather data at specified angle intervals.

(4) Azimuthal migration velocity analysis: the initial velocity field was established, based on the full-azimuth migration velocities and anisotropic parameters obtained in step (2), and this field was used to conduct migration velocity analysis for each azimuth.

(5) Ellipse fitting of anisotropic velocities: after the velocity ellipses were fit for the same reflection points at different azimuths, the fitting velocity function was used to calculate the migration travel time (Tsvankin and Thomsen, 1995).

(6) Pre-stack time migration of full-azimuth PS-waves: within the full-azimuth data gather, the velocity ellipses were used to calculate the migration velocities that corresponded to different azimuthal data, after which pre-stack time migration processing was performed based on the azimuthal velocities.

Correction method for S-wave splitting due to azimuthal anisotropy

We assumed that subsurface joints and seismic wave fields satisfy the following criteria: (1) only one group of joints exists in any analysis time window; (2) joints are vertical HTI-media features; and (3) the reflected wave in the analysis time window only comprises the fast and slow S-wave components. The principle governing the development of joint orientations within subsurface media was obtained following a suitable mathematical method (Alford, 1986; Gaiser, 1999) to further separate the wave fields of the fast and slow S-wave components (Figure 2).

The main objective of the HTI-media converted-wave anisotropic correction method is to employ a mathematical technique (Alford, 1986) to correct the propagation energies and moveouts of the R and T components. Before correction, the fast S-wave, (S_1), and slow S-wave, (S_2) , components were separated based on the PS-wave, and then the azimuth of the fracture strike was obtained. Then, in the target formation range of the HTI medium, the propagation moveout between the fast and slow S-wave components, $t = t_2 - t_1$, was computed based on the correlation between the seismic gathers, S_1 and S_2. An upward moveout shift was then performed for the slow S-wave seismic gather, in which S_2 was shifted toward zero-time by an increment of t. Finally, the corrected radial component, R'', and the corrected horizontal component, T'', of the PS-waves were calculated as

$$\begin{bmatrix} R'' \\ T'' \end{bmatrix} = M(\theta)\begin{bmatrix} S_1 \\ S_2 \end{bmatrix} = \begin{bmatrix} \cos\theta & \sin\theta \\ -\sin\theta & \cos\theta \end{bmatrix}\begin{bmatrix} S_1 \\ S_2 \end{bmatrix} \quad (3)$$

Equation (3) captures the core mathematical expression of the PS-wave correction:

$$\theta \in \left(-\frac{\pi}{2}\right], M(\theta) = \begin{bmatrix} \cos\theta & \sin\theta \\ -\sin\theta & \cos\theta \end{bmatrix}.$$

This equation is based on S-wave splitting theory and the propagation behaviors of PS-waves in HTI media. Based on the azimuthal pre-stack seismic data, the shear wave splitting technique was used to obtain the fast and slow S-wave components, as well as their propagation moveouts. These were then used to conduct moveout compensation corrections for the PS-wave R and T components (Simmons, 2009), thereby accomplishing an azimuthal anisotropic correction for improved converted-wave imaging. The layer-stripping method was used during the processing of real data to extract the propagation moveouts of fast S-wave and slow S-wave components along geological horizons. Consequently, corrections for converted-wave multi-layer anisotropic strata can effectively eliminate the adverse impacts of subsurface anisotropy on the seismic imaging of highly precise geological cross sections.

In summary, our anisotropic correction method based on PS-waves comprised three steps:

(1) The fast and slow S-wave components were

separated using the PS-wave R and T components, and their propagation moveouts were calculated.

(2) The R and T components were rotated using equation (3) to correct the energy and moveout of the R component.

(3) For anisotropic strata, the processing was conducted one horizon at a time via the first two steps until a precise seismic imaging result was obtained.

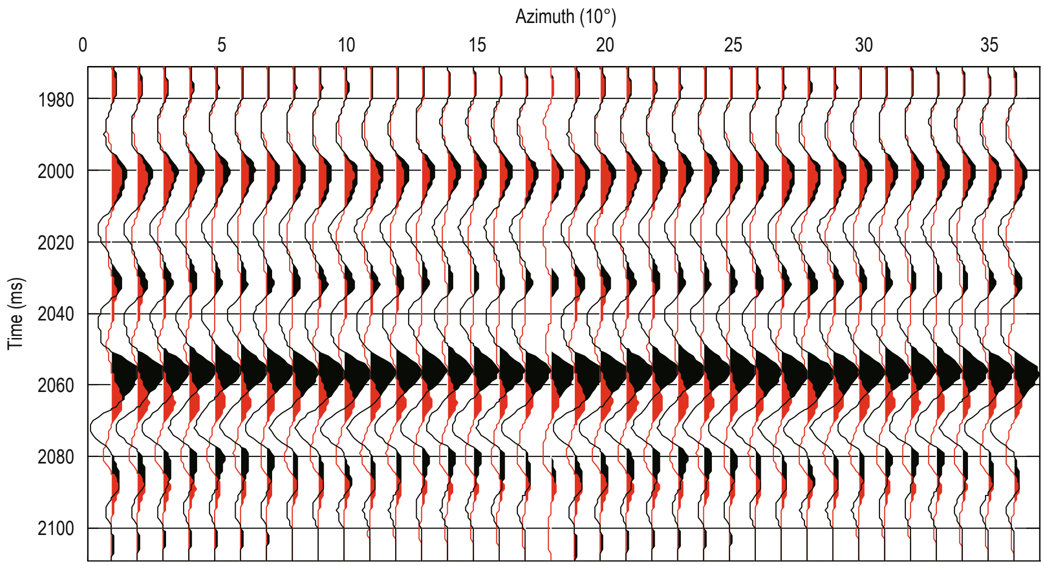

Fig. 2 Results of separating the fast S-wave (black) and slow S-wave (red) components using synthetic data.

We conducted a correction for the R and T components based on the fast and slow S-wave components that were split using the aforementioned PS-wave anisotropic correction method. The newly obtained PS-wave R and T components are plotted in Figure 3, in which the amplitude, frequency, and propagation time of the PS-wave R component show no changes; this is characteristic of horizontally layered isotropic media. The horizontally uniform features of the reflection events delineate the interfaces of the isotropic horizontal layers, which had uniform thicknesses. Due to the energy allocation effect of the S-wave splitting process, significant reflected energies were observed on the T component (Figure 3a). After correction, however, most of the energy was correctly reallocated to the R component, after which the T component exhibited no reflections along the interfaces (except for some noise), which is characteristic of the seismic response in an isotropic medium. In summary, due to the HTI strata, the R and T components initially exhibited the seismic response features of anisotropic media. After S-wave splitting and anisotropic corrections, the influences of the second, fourth, and sixth HTI strata were eliminated, bringing them in line with the seismic response features of isotropic media.

Our experimental processing of converted-wave seismic data with a theoretical model has verified the effectiveness of the fast and slow S-wave splitting method, as well as the converted-wave anisotropic correction method for the R and T components while demonstrating the significance of fracture response features and anisotropic corrections of converted waves.

Application case study with field data

The Western Sichuan Depression in China is extensively underlain by a tight clastic gas reservoir, and it contains numerous horizons at a variety of depths. Vertically, a near-source Upper Triassic gas reservoir is located within the same strata series as the source rock, and a number of Jurassic gas pools are situated far from the major source rock. The favorable reservoir-forming geological conditions of the Western Sichuan Depression include an abundant gas source characterized by a high-pressure anomaly, a regional paleo-uplift belt, a favorable storage-cap combination, good dredging conditions, and numerous complex traps. To date, many gas fields, including the Xinchang, Hexingchang, Pingluoba, Qiongxi, Zhongba, and Bajiaochang gas fields, have been discovered in the shallow, middle, and deep strata of the Western Sichuan Depression. Multiple high-productivity industrial gas wells, including Well

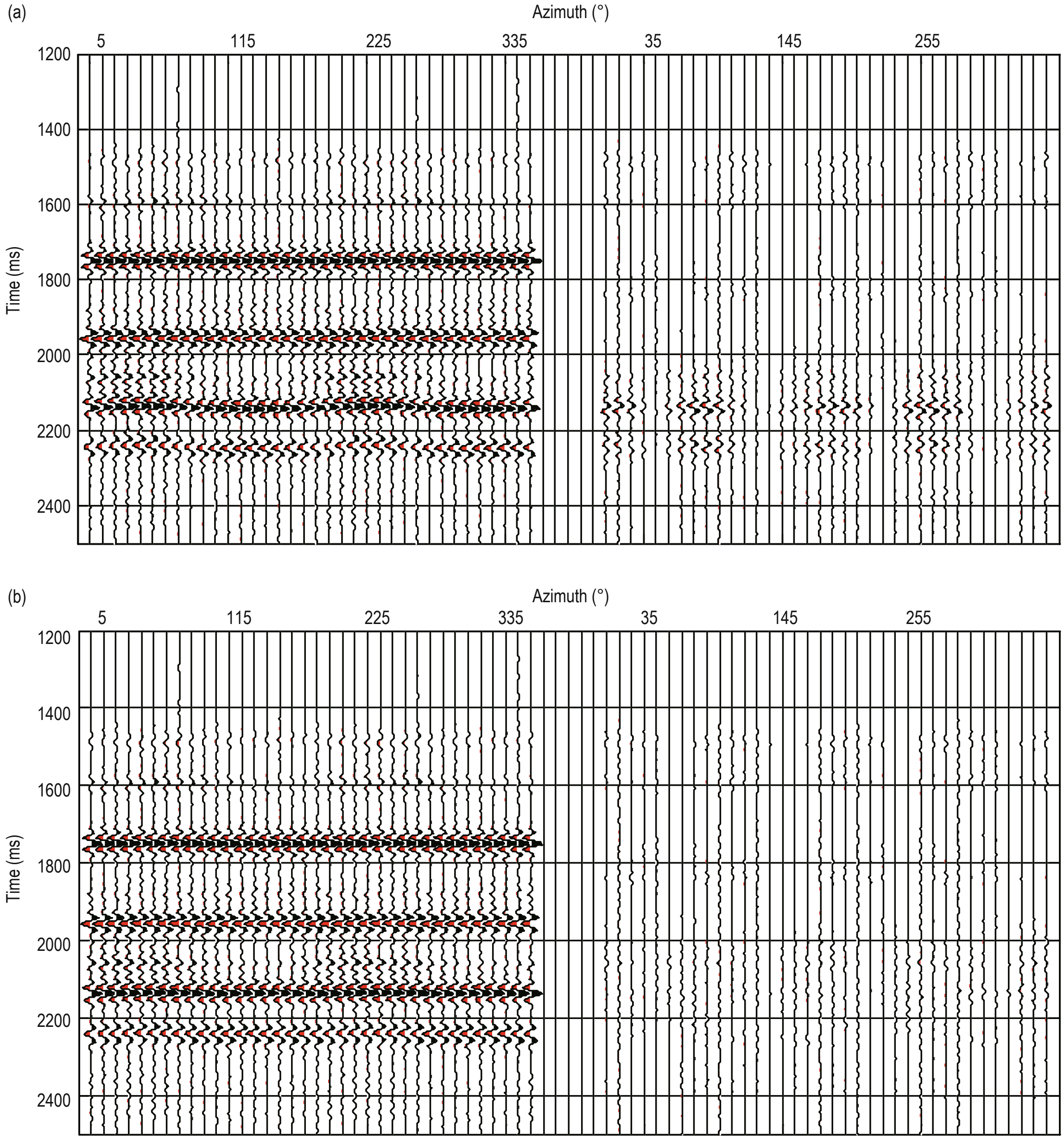

Fig. 3 (a) R component (left) and T component (right) before application of the S-wave splitting correction; (b) R component (left) and T component (right) after the S-wave splitting correction, as implemented on synthetic data.

X851, Well X856, Well X2, Well CG561, and Well DY1, have been successfully drilled in the Triassic Xujiahe Formation within the Xinchang structural belt to confirm the discovery and development prospects of tight sandstone gas reservoirs in the deep continental facies beneath the Western Sichuan Depression. However, gas exploration in this area is difficult because of the low porosity of the rock matrix, the tightness of the reservoir rock, and the development of fractures in the reservoirs of the Xinchang-Hexingchang region (Figure 4). In particular, these fractures have induced anisotropic characteristics in the reservoir, including inhomogeneous gas accumulation and apparent anisotropic PS-wave responses that have complicated imaging efforts. Figure 5 illustrates the PS-wave propagation in the Xinchang-Hexingchang area. The propagation times and amplitudes of the R component vary with the azimuth within the target stratum, whereas the T component registered high energy within the target stratum with obvious polarity reversals at every 90° interval. This indicates the presence of strong anisotropy and a high probability of fracture development in the strata. Consequently, the imaging result will be affected if the anisotropy is not effectively corrected. To obtain high-precision converted-wave imaging data, the HTI-media pre-stack time migration and the anisotropic correction methods were used as described above for the three-dimensional and three-component (3D3C) seismic anisotropic processing of the research area. High-quality seismic data were acquired with continuous reflected wave groups, distinct structural features, and specific stratigraphic inter-relationships that helped establish a firm data foundation for the exploration of the complex, hidden gas reservoirs in the area.

Fig.4 Formation fracture imager photo and core photos from Well CX560.

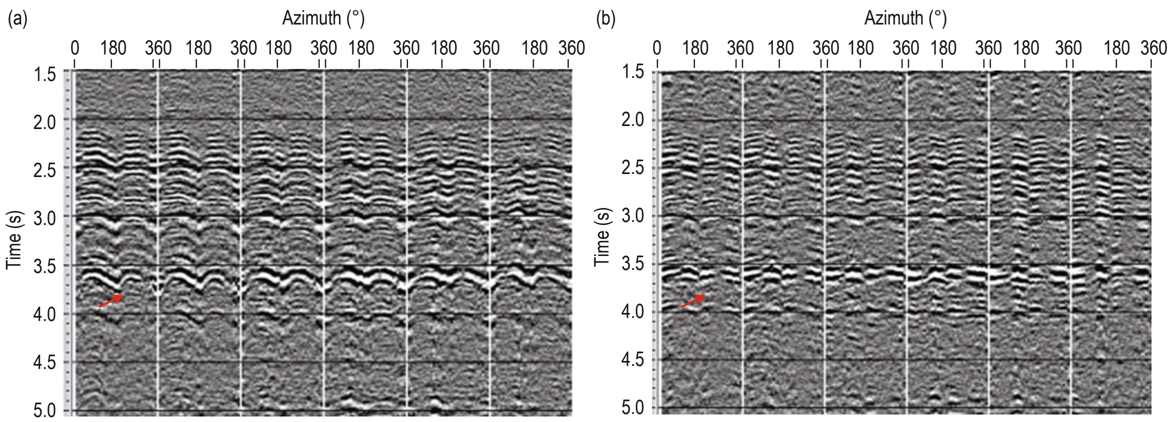

Fig.5 Azimuthal stacked gathers of the R component (a) and T component (b) in the 3D3C work area of the Xingchang-Hexingchang region in the Western Sichuan Depression. The red arrows indicate the target stratum in each image.

To obtain high-precision PS-wave images, the isotropic-, VTI-, and HTI-media imaging methods were applied to the PS-wave pre-stack seismic data to acquire distinctly different processing results. Figure 6 shows a comparison between the isotropic media and anisotropic HTI-media cases. The velocity updating method based on isotropic media was unable to effectively “flatten” the PS-wave seismic gathers. This is because the velocity anisotropy of the PS-waves resulted in an uplift or pull-down event within the pre-stack time migration gather, which was not easily corrected and which inevitably affected the subsequent stacked images. However, in our HTI-media imaging method, the gathers were significantly flattened through velocity anisotropy processing. The post-flattening PS-wave seismic gathers reflected the true AVO response features of reservoirs during the subsequent stacked imaging.

Similarly, the VTI-media imaging method failed to produce ideal migration results in the early stages, whereas the HTI-media imaging method worked better for actual subsurface media features. Figure 7 shows a comparison between the converted-wave VTI- and HTI-media processing results. They exhibit the same structure and shape, but the HTI-media processing was better during the relatively stable and continuous PS-wave reflection events. This confirms that the HTI-media-based anisotropic processing method offers a higher resolution, a better signal-to-noise ratio, and richer

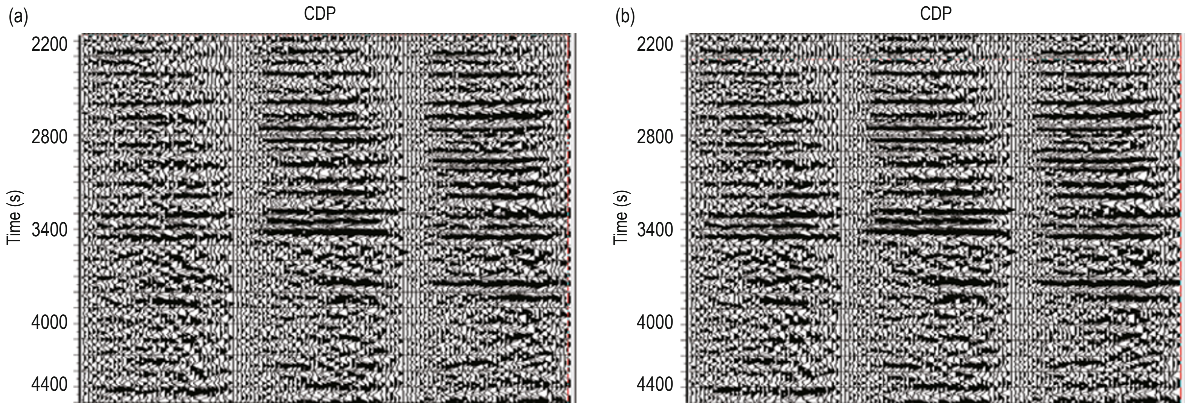

Fig.6 Comparison of pre-stack time migration gathers for isotropic media (a) and anisotropic HTI-media (b).

strata information. The obtained section is favorable for thin-layer identification and interpretation, structural interpretation, strata tracking, and reservoir prediction.

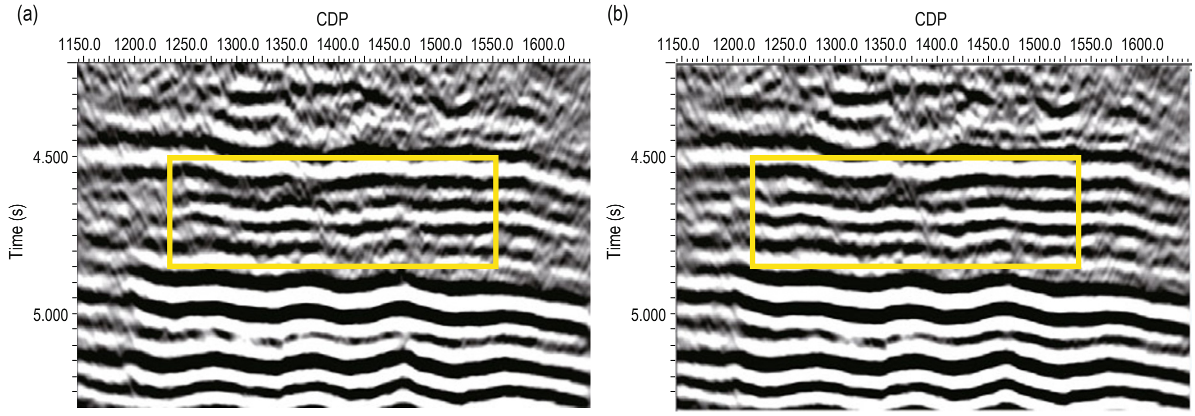

Fig.7 Comparison of converted-wave migration imaging effects for the VTI-media (a) and HTI-media (b). The yellow boxes highlight a region with improved results for the HTI-media imaging.

Figure 8 shows a comparison of S-wave splitting results before and after anisotropic correction. Figure 9a and 9b illustrate the R and T components before the correction, respectively. Due to the effects of S-wave splitting, the reflection events in the R component undulated, whereas the corresponding T component events had more reflection energy. Figure 9c and 9d show the R and T components after the correction,

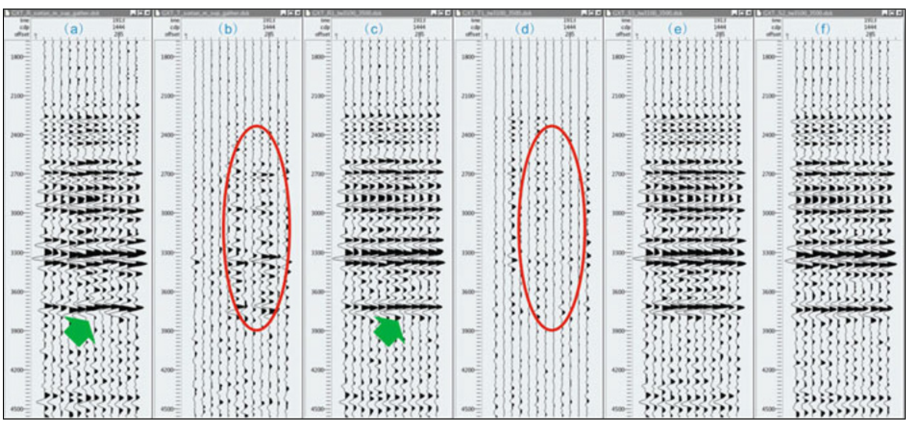

Fig.8 Comparison between the S-wave splitting of PS-wave R and T components before and after anisotropic corrections (from left to right: original R and T stacked data; R and T stacked data after S-wave splitting; fast and slow S-wave stacked data).

respectively. The event moveout in the R component was removed by the correction, and the energy of the T component was reallocated to the R component through rotation. Finally, Figure 9e and 9f demonstrate the extracted fast and slow S-wave components, respectively, based on the R and T components, and a distinct propagation moveout can be seen.

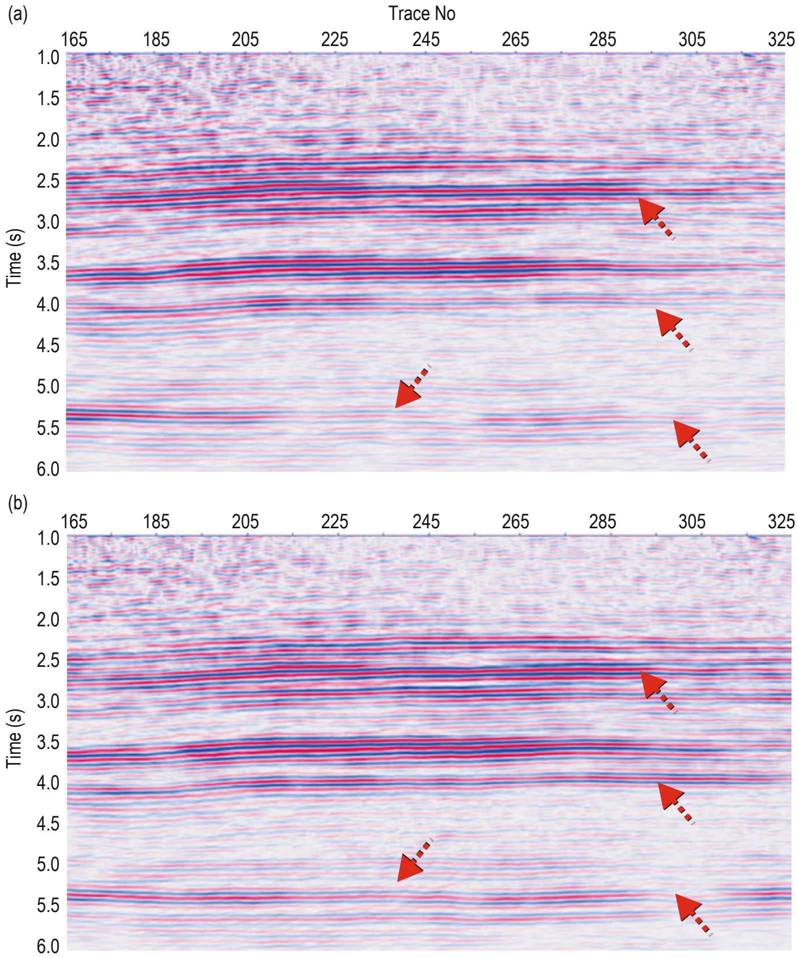

Fig. 9 Comparison of stacked sections of PS-wave splitting azimuthal anisotropy as it appeared before (a) and after (b) anisotropy correction. Red arrows indicate points of particular improvement or interest.

After the anisotropic correction was applied, based on the HTI-media method, the energy on the T component was effectively reallocated to the R component, the S-wave splitting phenomenon was effectively handled, and the PS-wave imaging quality was further improved. Figure 9 shows a comparison of the stacked sections of the PS-wave splitting azimuthal anisotropy, both before and after the correction. The results indicate that the reflection event energies and frequencies after the azimuthal anisotropic correction were more consistent and that the imaging quality at each depth was improved, as is evidenced by the relatively continuous strata reflections and clearer structural features. These findings suggest that our processing approach can provide a better-quality data base for late-stage reservoir interpretation.

Conclusions

The following conclusions can be drawn from our in-depth testing of pre-stack migration and anisotropic correction methods for PS-waves in HTI media, as well as through the processing of PS-wave seismic field data from the Xinchang-Hexingchang region of the Western Sichuan Depression:

(1) Through theoretical research and synthetic data processing, we confirmed that both velocity anisotropy and S-wave splitting should be considered during the

processing and migration imaging of HTI media to ensure accurate geological interpretation and reservoir prediction. When subsurface joints are well-developed, the fast and slow S-wave components that split from PS-waves can have an apparent impact on the R and T component reflection events. Thicker strata will generate a larger moveout delay and have a greater impact on the converted-wave imaging quality.

(2) The deep, tight reservoir fractures in the strata beneath the Western Sichuan Depression result in distinct structural anisotropy. This gives rise to the directional dependence of the energy and travel time of the PS-wave R component. Meanwhile, the T component exhibits an energy response and a 90° phase reversal. Our isotropic- and VTI-media imaging methods failed to yield satisfactory image qualities in the early stages. However, the PS-wave anisotropy was effectively corrected by employing our HTI-media processing method. In addition, the pre-stack gathers were precisely flattened, and the S-wave splitting effect was eliminated. Furthermore, the T component energy was rotated and reallocated to the R component, which improved the imaging of the latter.

In conclusion, HTI media conform to a fractured-media model that is relatively similar to the actual conditions of the subsurface. With the application of pre-stack migration imaging processing and an anisotropic correction method based on the propagation rules of PS-waves in HTI media, the adverse effects of S-wave splitting can be effectively eliminated and the imaging precision can be improved. After applying these methods to a set of 3D3C seismic data that were collected from the Xinchang-Hexingchang region of the Western Sichuan Depression, high-quality seismic data with continuous, reflected wave groups, distinct structural features, and specific stratigraphic contact relationships were obtained. These findings should provide vital technological support for the exploration of complex, hidden gas reservoirs in the area.

References

Akalin, M. F., Muhamad, A.A., Tan, Y.C., et al., 2014, 3D-PS converted waves-solving 3D-imaging challenges under gas clouds-offshore Malaysia: 76th EAGE Conference & Exhibition, Extended Abstracts, Tu D202 03.

Alford, R. M., 1986, Shear data in the presence of azimuthal anisotropy: 56th Annual International Meeting, SEG, Expanded Abstracts, 476−479.

Berryman, J. G., 2009, Aligned vertical fractures, HTI reservoir symmetry and Thomsen seismic anisotropy parameters for polar media: Geophysical Prospecting, **57**(2), 193−208.

Chang, C. H., Chang, Y. F., Tseng, P. Y., 2017, Azimuthal variation of converted-wave amplitude in a reservoir with vertically aligned fractures - a physical model study: Geophysical Prospecting, **65**(1), 221−228.

Chen, H. F., Li, X. Y., Qian, Z. P., et al., 2016, Prestack migration velocity analysis based on simplified two-parameter moveout equation: Applied Geophysics, **13**(1), 135−144.

Cheng, B. J., and Xu, T. J., 2009, Application of converted wave data in reservoir prediction for Chuanxi depression: Geophysical Prospecting for Petroleum (in Chinese), **48**(02), 181−186.

Cheng, J. B., Wang, T. F., Wang, C. L., and Geng, J. H., 2012, Azimuth-preserved local angle-domain prestack time migration in isotropic, vertical transversely isotropic and azimuthally anisotropic media: Geophysics, **77**(2), S51−S64.

Crampin, S., and Peacock, S., 2005., A review of shear-wave splitting in the compliant crack-critical anisotropic earth: Wave Motion, **41**(1), 59−77.

Dai, H. C., and Li, X. Y., 2005, Accuracy of a simplified moveout formula for PS converted–waves in multi-layered media: 75th Annual International Meeting, SEG, Expanded Abstracts, 1010−1014.

Dai, H. C., and Li, X. Y., 2006, The effects of migration velocity errors on travel time accuracy in prestack Kirchhoff time migration and the image of PS converted waves: Geophysics, **71**(2), S73−S83.

Dai, H. C., and Li, X. Y., 2007a, Velocity model updating in prestack Kirchhoff time migration for PS converted waves Part I–Theory: Geophysical Prospecting, **55**(4), 525−547.

Dai, H. C., and Li, X. Y., 2007b, Velocity model updating in prestack Kirchhoff time migration for PS converted waves Part II–Application: Geophysical Prospecting, **55**(4), 549−559

Dai, H. C., and Li, X. Y., 2008a, A practical approach to compensate for diodic effects of PS converted waves. 78th Annual International Meeting, SEG, Expanded Abstracts: pp. 3053-3057.

Dai, H. C., and Li, X. Y., 2008b, Effect of errors in the migration velocity model of PS-converted waves on travel time accuracy in prestack Kirchhoff time migration in weak anisotropic media: Geophysics, **73**(5), S195−S205.

Dai, H. C., and Li, X.Y., 2011, Fracture detection using

PS converted waves: A case study from Daqing oil field: 81stAnnual Meeting, SEG, Expanded Abstracts, 1318−1322.
Dai, H. C., Li, X. Y., and Conway, P., 2004, 3-D prestack Kichh off time migration of PS-waves and migration velocity model building: 74th Annual International Meeting, SEG, Expanded Abstracts, 2227−2230.
Gaiser, J. E., 1999, Applications for vector coordinate systems of 3-D converted wave data: The Leading Edge, **18**(11), 1290−1300.
Huang, Z. Y., and Wang, Y. J., 2014, An effective 3D PS-wave true-amplitude prestack time migration method: Geophysical Prospecting for Petroleum (in Chinese), **53**(04), 431−436.
Huang, Z. Y., Qu, S. L., Wang, Y. J., et al., 2009, Kirchhoff prestack time migration of PS-wave data for the layered anisotropic medium: Chinese Journal of Geophysics (in Chinese), **52**(12), 3109−3115.
Jenner, E., 2011, Combining VTI and HTI anisotropy in prestack time migration: Workflow and data examples: The Leading Edge, **30**(7), 732−739.
Koren, Z., and Ravve, I., 2014, Azimuthally dependent anisotropic velocity model update: Geophysics, 79(2), C27−C53.
Li, H.Q., Lin, W., Lu, Z. W., et al, 2015, Azimuth anisotropy moveout removal based on difference: Oil Geophysical Prospecting (in Chinese), **50**(06), 1112−1117.
Li, X. M., Chen, S. Q., and Li, X. Y., 2013, The analysis and application of simplified two-parameter moveout equation for C-waves in VTI anisotropy media: Applied Geophysics, **10**(4),477−87.
Li, X. Y., and Yuan, J. X., 2003, Converted-wave moveout and convrsion-point equations in layered VTI media: theory and application: Journal of Applied Geophysics **54**(3), 297−318.
Li, X. Y., and Yuan, J. X., 2005, Converted-wave seismology in anisotropic media revisited, part I: basic theory: Applied Geophysics, **2**(1), 26—40.
Mahmoudian, F., Margrave, G. F., Wong, J., and Henley, D. C., 2015, Azimuthal amplitude variation with offset analysis of physical modeling data acquired over an azimuthally anisotropic medium: Geophysics, **80**(1), C21−C35.
Qian, Z. P., Zhang, S. H., Zhao, B., et al., 2012, Numerical modeling of PP- and PS-wave azimuthal anisotropy in HTI media: Applied Geophysics, **9**(4), 429−439.
Simmons, J. L., 2009, Converted-wave splitting estimation and compensation: Geophysics, **74**(1), D37−D48.
Skopintseva, L., and Alkhalifah, T., 2013, An analysis of AVO inversion for postcritical offsets in HTI media: Geophysics, **78**(3), N11−N20.
Sun, C. W., and Martinez, R. D., 2003, 3D Kirchhoff PS-wave prestack time migration for V(z) and VTI media: 73rd Annual International Meeting, SEG, Expanded Abstracts, 957−960.
Thomsen, L., 1986, Weak elastic anisotropy: Geophysics, **51**(10), 1954−1966.
Thomsen, L., 1999, Converted-wave reflection seismology over inhomogeneous anisotropic media: Geophysics, **64**(3), 678−690.
Tsvankin, I., and Thomsen, L., 1995, Inversion of reflection traveltimes for transverse anisotropic: Geophysics, **60**(4), 1095−1107.
Zhang, L. Y., Liu, Y., Chen, X. H., 2009, Converted wave amplitude-preserving prestack migration by pseudo-offset migration: Journal of China University of Petroleum (in Chinese), **33**(05), 50−55.
Zhang, L. Y., Wang, Y. C., and Pei, J. Y., 2015, Three-component seismic data in thin interbedded reservoir exploration: Applied Geophysics, **12**(1),79−85.

Yan Li-Li. is a Ph.D. student studying Quaternary geology at the Chengdu University of Technology. Her research interests are seismic wave propagation theory and application technology, geological structures and Quaternary environments.

Cheng Bing-Jie is an associate professor at the Chengdu University of Technology. She obtained her bachelor's degree in applied geophysics from the China University of Geosciences (Wuhan) in 2000 and received a master's degree in Earth exploration and information technology from the same university in 2003. She received her PhD from the Institute of Geology and Geophysics of the Chinese Academy of Sciences in 2007. Her main research interests are seismic anisotropy analysis, multi-component seismic exploration, and reservoir prediction methods.

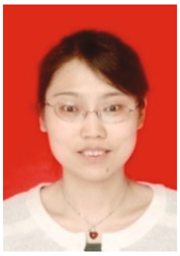

(Edited by Liu Yang)